01 Apr 2007

Microwave and Millimeter Wave Nondestructive Testing and Evaluation -- Overview and Recent Advances

Sergey Kharkovsky
Missouri University of Science and Technology

R. Zoughi
Missouri University of Science and Technology, zoughi@mst.edu

Recommended Citation

S. Kharkovsky and R. Zoughi, "Microwave and Millimeter Wave Nondestructive Testing and Evaluation -- Overview and Recent Advances," *IEEE Instrumentation and Measurement Magazine*, vol. 10, no. 2, pp. 26-38, Institute of Electrical and Electronics Engineers (IEEE), Apr 2007.
The definitive version is available at https://doi.org/10.1109/MIM.2007.364985

Microwave and Millimeter Wave Nondestructive Testing and Evaluation

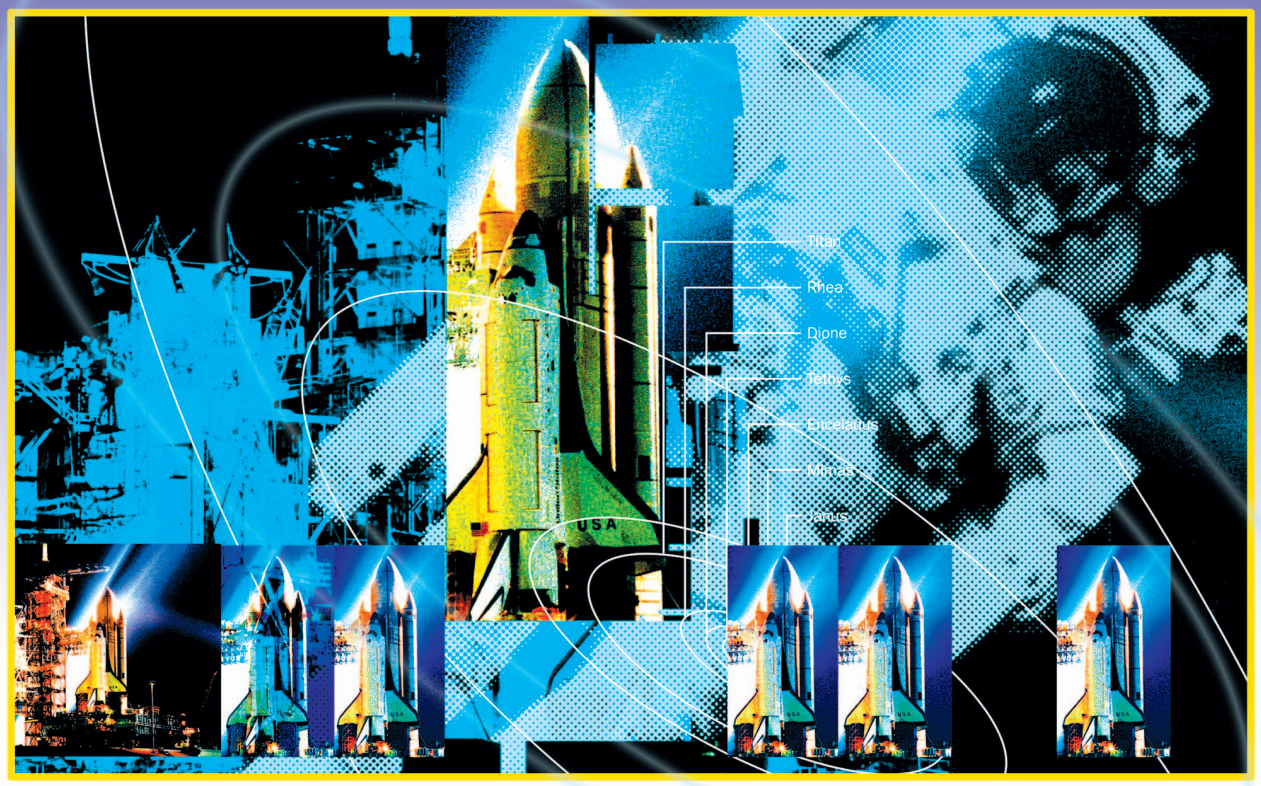

Overview and Recent Advances

Sergey Kharkovsky and Reza Zoughi

Nondestructive testing and evaluation (NDT&E) is the science and practice of evaluating various properties of a material without compromising its utility and usefulness [1]. Those material properties might be physical, chemical, mechanical, or geometrical. The interrogating signal must be suitable for use in a laboratory or test situation and be able to interact with the material under test. The existing standard techniques for NDT&E methods may not always be capable of inspecting the new composites that are replacing metals in some applications. Microwave and millimeter wave NDT&E techniques are recognized as tools that render a more comprehensive picture of an inspection problem. Electromagnetic signals at microwave and millimeter wave frequencies are well suited for inspecting dielectric materials and composite structures in many critical applications [2].

This article focuses on three recent applications of microwave and millimeter wave NDT&E techniques that involve novel instrumentation development and measurements, including:

- disbond detection in strengthened concrete bridge members retrofitted with carbon fiber reinforced polymer (CFRP) composite laminates,
- corrosion and precursor pitting detection in painted aluminum and steel substrates, and

1094-6969/07/$25.00©2007IEEE

- detection of flaws in spray-on foam insulation and the acreage heat tiles of the Space Shuttle through focused and synthetic imaging techniques.

These applications have been performed at the Applied Microwave Nondestructive Testing Laboratory (*amntl*) at the University of Missouri-Rolla.

Background

Usually, NDT&E is performed with an interrogating electric, magnetic, or acoustic signal. The signal interacts with the material, and the response gives properties of the material. The majority of well-established and "standard" NDT&E methods—used for a wide range of applications—are ultrasound, eddy current, shearography, magnetic particle testing, dye penetrant, visual testing, and radiography. [1] Every method has its own particular advantages, disadvantages, and realm of applicability. For example, ultrasonic signals may not penetrate inside highly porous materials and cannot interact with their inner structure. Eddy current methods do not work well when inspecting lossless dielectric materials in which eddy currents cannot be induced.

Materials technology has produced lighter, stiffer, stronger, and more durable electrically insulating composites which are replacing metals in many applications. These composites require alternative inspection techniques because the standard NDT&E methods may not be capable of inspecting them. In some cases, microwave and millimeter wave NDT&E techniques may be the only viable solution or can be used in combination with other methods to render a more comprehensive picture of an inspection problem.

Attributes of Microwave and Millimeter Waves NDT&E

The well-established microwave frequency spectrum spans from about 300 MHz to 30 GHz, while the frequency span of 30–300 GHz is associated with the millimeter wave spectrum; the corresponding wavelength ranges are 1,000-10 mm and 10 mm-1 mm, respectively [3]. Figure 1 shows the frequency and wavelengths associated with microwave and millimeter waves. Interrogating signals at these frequencies can readily penetrate dielectric materials and interact with their inner structure.

The utility of microwave and millimeter wave NDT&E has been applied to the following diverse applications:

- dielectric material characterization using a diverse array of techniques and for a wide range of applications including dielectric property characterization, dielectric mixture constituent determination, porosity evaluation in polymers, moisture measurements, cure monitoring of resin binders, rubber products and cement-based materials [5]–[23]
- detection and sizing of minute changes (in the range of a few μm) in thickness of dielectric sheet materials (including conveyed products), and detection of small voids and thin disbonds and delaminations in stratified (sandwich) composites and estimation of their locations [24]–[32]
- fatigue crack detection and sizing in metal surfaces, including those under paint and thin dielectric coatings using several unique approaches and detection of other surface anomalies in metals [4], [33]–[44]
- detection and evaluation of corrosion under paint and composite laminates, including detection of corrosion precursor pitting [45]–[49]
- near-field, focused, and synthetic aperture microwave and millimeter wave imaging for flaw detection and evaluation in various composite structures [15], [29], [32], [50]–[59]
- biological applications [60]–[66]
- microwave microscopy [67]–[69]
- composites [2], [4]
- new applications being discovered continuously.

When applying microwave and millimeter wave NDT&E methods in near-field applications, there are a number of advantages. Such advantages include the fact that these methods are

- noncontact
- one-sided
- do not require a couplant to transmit the signal into the material under test (unlike ultrasonic methods)
- mono-static
- low-power
- compact
- easily adaptable to existing industrial scanners
- real time
- in-field
- operator friendly
- do not require operator expertise in the field of microwave engineering
- enable images with high resolutions to be obtained since in the near-field the spatial resolution is a function of the probe dimensions (which in these frequency ranges are quite small) and not the operating wavelength
- robust, rugged, and repeatable
- relatively inexpensive.

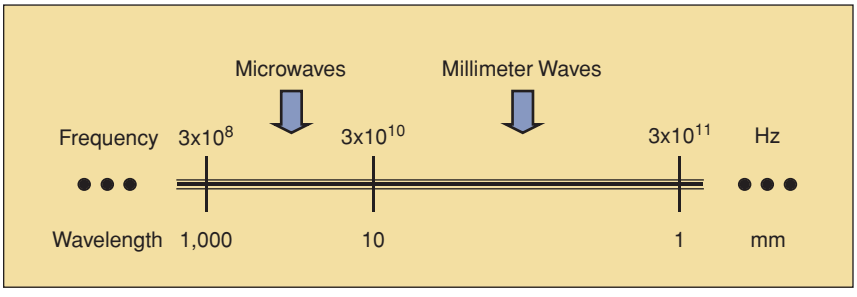

Fig. 1. Microwave and millimeter wave frequency ranges and associated wavelengths (not to scale).

In addition, measurement parameters such as frequency, bandwidth, polarization, phase, and magnitude information (coherent properties) and probe properties can be optimized for a particular application. This optimization may be performed experimentally or theoretically [2].

In many applications, it is best to first perform a theoretical optimization so that the optimal measurement parameters of interest can be chosen in the subsequent experimentation. The standoff distance (distance between the probe and the material under test, sometimes known as liftoff [1]) is a significant parameter that can render measurement results with extreme sensitivity (for example, see [31]). If it is not chosen optimally, or if it changes during a particular measurement, the results are often significantly and adversely affected. Therefore, even though near-field measurements provide for a wide range of measurement parameters (i.e., increased measurement degrees of freedom), the choice of these parameters (separately or collectively) is an important consideration.

Throughout this article, two techniques are used. For one technique, a sample is placed on a two-dimensional (2-D) scanning table under computer control and an inspection system is held at a certain distance above it. For the other technique, the system is attached to a 2-D scanning mechanism held above a sample while it is scanned. The system output voltage produces a raster scan or a 2-D image of the sample. The measured output voltages are then normalized and assigned different grayscale or color levels in the image that is produced.

Inspection of CFRP Composite Laminate-Strengthened Structural Members

CFRP composites are being used more in rehabilitating infrastructures of existing structures as well as in new bridge construction [70]–[72]. CFRP composites are bonded externally to concrete members to provide additional flexural, shear, or confining reinforcement since they are strong, lightweight, and not susceptible to corrosion. The use of CFRP for strengthening structural members like bridge girders and bents is very attractive since this process is inexpensive and rapid and does not disrupt traffic flow.

In this process, it is extremely important to validate the quality of the retrofit at the time of installation and during service to ensure strength. The effectiveness of the retrofit may be significantly diminished if a large section of the CFRP laminate becomes disbonded from the structure. Disbonds between a CFRP laminate and concrete may occur due to a variety of reasons, including improper application of the laminate, presence of moisture near the concrete surface, and impact damage. Currently, the most prominent on-site methods for detecting disbonds and other defects or anomalies such as cracks, impact damages, fiber breakages, and fiber misalignment are visual inspection and tap testing. However, some disbonds may be invisible to visual inspection and/or may be small, but they may still cause significant degradation of strength.

There is a great need for developing a robust nondestructive inspection technique that can reliably detect the presence of various anomalies in CFRP-retrofitted structures. Several NDT&E techniques, including microwave techniques [73]–[84], have been considered and attempted for inspecting CFRP composites for the presence of disbonds, concrete damage, and fiber misalignment.

CFRP laminates have two properties that dictate the NDT&E techniques applied to them. They contain carbon, which is highly conductive at microwave frequencies, and they are commonly unidirectional to provide additional strength in a particular direction. The technique must include an optimal choice of standoff distance (as explained earlier) and considerations regarding the change in this parameter due to surface roughness and shaking caused by traffic flow or improper assembly of the measurement and scanning platform on a bridge member (e.g., a bent). Second, the anisotropy associated with unidirectional CFRP laminates causes microwave signals to totally reflect off the laminate when the fiber directions and the electric field polarization vector are parallel to each other (parallel polarization). The signal penetrates into the laminate when the electric field polarization is perpendicular to the fiber directions (perpendicular polarization). Thus, the choice of polarization is very important. In both cases, the reflected signal can be used to generate 2-D raster images of an area.

The perpendicular polarization case is well-suited for detecting and evaluating disbonds and concrete damages hidden by CFRP. The parallel polarization provides information about surface roughness, fiber breakage in the CFRP, changes in standoff distance during inspection, etc. (since the signal in this case only provides information about standoff distance). Therefore, the information from parallel polarization can be used to remove the undesired influence of surface roughness and standoff distance change from the data obtained from perpendicular polarization.

We developed a novel near-field microwave inspection system employing a dual-polarized near-field microwave reflectometer [84]. A reflectometer is a microwave circuit capable of transmitting a microwave signal at a particular frequency and polarization and receiving the subsequent reflected signal. Its output is proportional to the magnitude or phase or both of the reflected signal. This system is capable of automatic removal of the influence of undesired standoff distance (or surface roughness) variations. It can simultaneously generate three raster images of a defect: two at orthogonal polarizations and one after the influence of standoff distance variations is removed using the information provided by the parallel polarization images.

Subsequent to designing and constructing this system at X-band, it was extensively tested in the laboratory and in the field on an actual bridge in Dallas County, Missouri [84]. Several 600 × 600 mm CFRP patches were bonded to the abutment and the bent of this bridge. A number of artificial disbonds (subtle and severe) were manufactured in them by injecting air between the CFRP patches and the concrete

members (the patches were later painted to visually blend into the bridge). In addition, several very small and subtle but unintentional disbonds were also produced in these patches. Figure 2 shows one of the bent patches while being tested by the dual-polarized reflectometer attached to a computer-controlled scanning platform. Figure 2 also shows the three microwave images of the 270 × 330 mm scanned area of the CFRP patch in the laptop display. Close-up views of these images are shown in Figure 3. The dark and bright indications in the perpendicular polarization image in Figure 3(a) represent different disbonds and influence of surface roughness and any bulging that may be present as a result of air injection. The indications of the slight surface bulging and depressing due to the presence of air between CFRP and concrete and the surface roughness are also clearly visible in the image for parallel polarization [Figure 3(b)]. The compensated image [shown in Figure 3(c)] was produced (in real-time) by removing the effect of bulging and standoff distance variation using the information from Figure 3(b) and removing it from the data in Figure 3(a). Figure 3(c) clearly shows the disbonds as well as the local nonuniformity associated with them. The locations and sizes of the detected disbonds (indicated by this compensated image) in all of the investigated cases agreed well with their actual locations and sizes on the bonded CFRP patch, and the results were further corroborated by tap testing.

Fig. 2. The dual-polarized microwave reflectometer attached to a scanning platform while inspecting a CFRP patch bonded to the bent of a bridge.

This versatile dual-polarized reflectometer system is clearly a robust system for performing on-site measurements. These and many other results from different patches have clearly shown the effectiveness of this novel system as a life-cycle inspection tool for detecting and evaluating disbonds in CFRP-strengthened structural members and other similar composites.

Detection and Evaluation of Corrosion and Precursor Pitting Under Paint

Naval vessels and critical aircraft structural components such as wings and fuselages are continuously exposed to harsh environments that vary considerably in temperature and moisture content. These varied environmental conditions lead to corrosion of these components and, in some cases, to accelerated corrosion. In most cases, the corrosion is hidden under paint and primer and cannot be visually detected. Thus, detection is only possible when corrosion becomes severe and causes blistering of the paint. When this happens, a relatively large area must be rehabilitated, which may require significant time, resources, and downtime.

The initiation of corrosion is preceded by the presence of corrosion precursor pitting. Detection of precursor pitting yields information about the susceptibility to corrosion

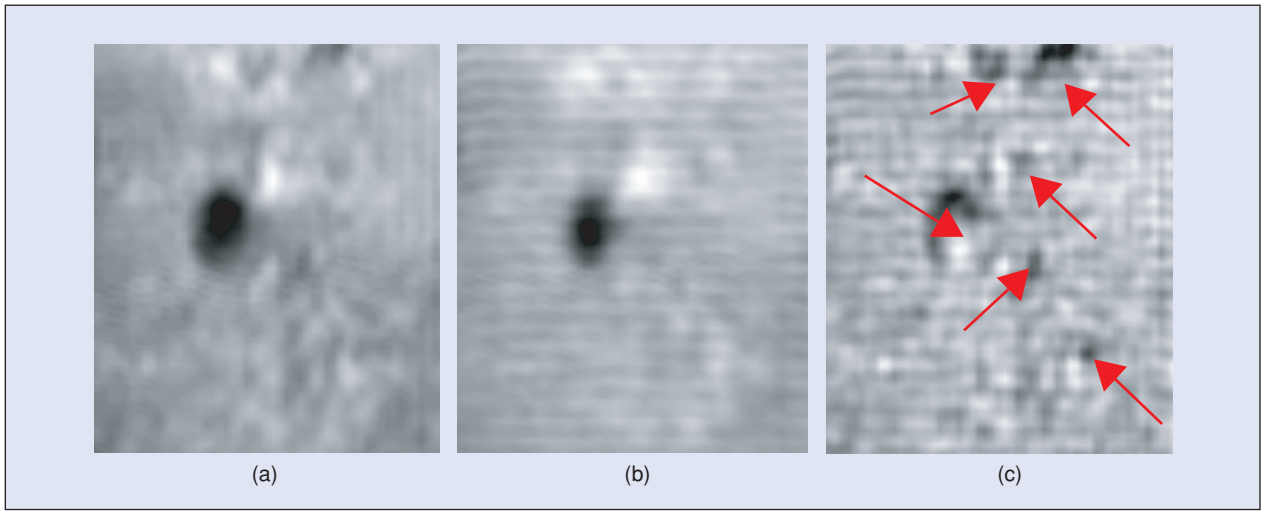

Fig. 3. Microwave images of the portion (270 x 330 mm) of the CFRP patch at (a) perpendicular polarization, (b) parallel polarization, and (c) compensated image (the detected disbonds are marked by red arrows).

initiation [85]–[87]. The size (area and depth) of a precursor pitting is naturally very small (i.e., fractions of a millimeter). When it becomes relatively large, the corrosion process has already initiated.

The dielectric properties of paint and primer are quite similar, while they are somewhat different than those of corrosion byproducts (aluminum and iron oxides). The dielectric properties of different paint and corrosion byproducts have been measured in the past, so that theoretical measurement parameter optimization could be conducted for the purpose of measurement parameter optimization [45]–[47]. As mentioned earlier, when operating in the near-field of a probe, slight variations in thickness and/or dielectric properties of thin dielectric coating such as paint and corrosion can be robustly detected and hence reveal the presence and severity of a corroded region.

The existing standard techniques for NDT&E methods may not always be capable of inspecting the new composites that are replacing metals in many applications.

Detection of Corrosion Under Paint in Steel Substrates

To demonstrate the capability of near-field microwave NDT&E methods for detecting and evaluating corrosion under paint, the results for a painted steel sample containing corrosion (under paint) are discussed here. It should be noted that similar samples made of aluminum have also been extensively investigated, and the reader is referred to [47], [48], and [88] for those cases. The current sample had a corrosion patch of 50 × 50 mm and a thickness of 0.05 mm, which was produced in a salt fog chamber. It had a primer thickness of 0.076 mm and paint thickness of 0.05 mm, as shown in Figure 4(a). This sample was extensively investigated at several frequencies and using different reflectometer systems. A 62-GHz (V-band) image of this sample, obtained using a phase-sensitive reflectometer and an open-ended rectangular waveguide probe, is shown in Figure 4(b) [89]. It should be noted that the thickness of the corrosion layer in this sample was relatively thin. Consequently, using microwave or lower-frequency millimeter wave signals did not render acceptable results. However, at higher millimeter wave frequencies, very clear images of the corroded area were obtained.

It is important to note that the image of the corroded area in Figure 4(b) also shows detailed nonuniformities associated with the corroded area, including indications of small pitting (i.e., the localized dark spots). Similar indications were originally obtained in a previous investigation, which subsequently indicated the capabilities of these methods for detecting tiny corrosion pitting [47]. This important subject will be discussed in the next section. Clearly, images obtained by these systems are capable of providing comprehensive information about the presence and properties of a corroded region. To this end, it is also important to note that using the available multilayered electromagnetic formulation (developed for inspection of layered composites [26]), one may also calibrate the measured results to obtain a good estimate of the corrosion thickness [90].

Detection of Corrosion Precursor Pitting

To demonstrate the capability of these methods for detecting corrosion precursor pitting, a set of laser-machined pittings with diameter and depth in the range of 200–400 mm was produced in an aluminum plate, as shown in Figure 5(a). To further improve the spatial resolution associated

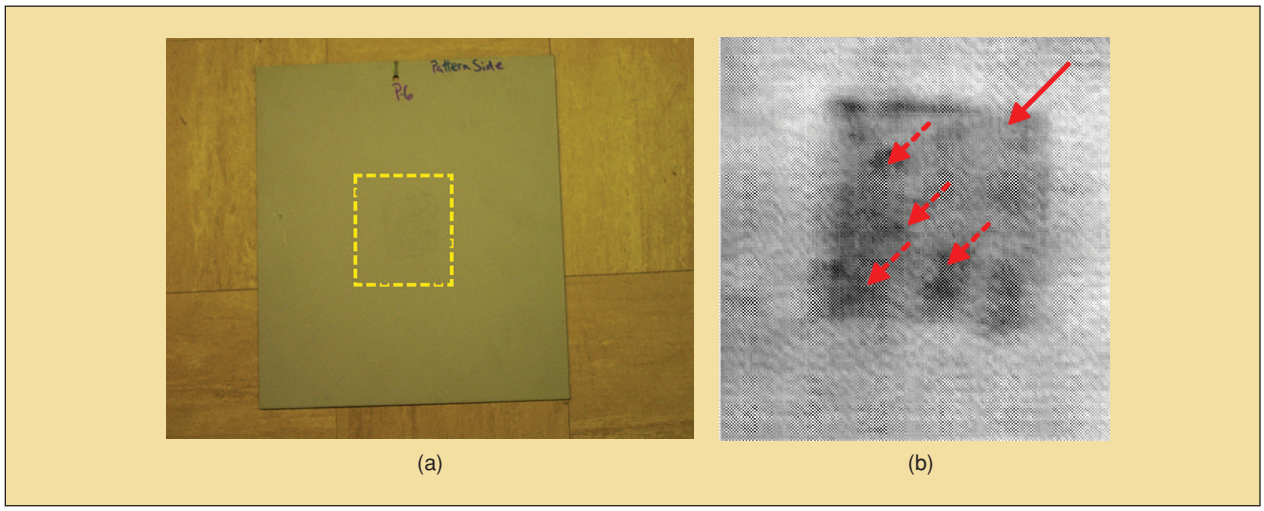

Fig. 4. (a) Picture of a steel sample with the marked scanned area and (b) image of the scanned area at 70 GHz (solid arrow shows the image of a square corrosion patch and dash arrows show the indications of pittings). Reprinted with permission from S. Kharkovsky and R. Zoughi from *Review of Progress in Quantitative Nondestructive Evaluation* 25B, AIP Conference Proceedings, vol. 820, 2006, pp. 1277–1283, Copyright 2006, American Institute of Physics.

with a V-band rectangular waveguide probe, the waveguide was loaded by a thin dielectric insert that tends to concentrate the probing electric field in a smaller region at the waveguide aperture. This probe was used to produce an image of the laser-pitted panel at 67 GHz. Figure 5(b) shows the results of this experiment by showing the relative dimensions of the pittings through the characteristics of the signal associated with each pitting. The information contained in this image can be used to get a reasonably close estimate of the pitting dimensions [90], [91]. It must be mentioned that the standoff distance was held fairly constant while scanning this plate. Slight variation in the standoff distance caused significant clutter and resulted in the inability to detect these pittings, since they are not only small but also since the probe used in this case—although high resolution—is inherently very sensitive to variations in standoff distance.

Therefore, to detect a pitting—in particular, when under paint—one must not only optimally choose the standoff distance but must also keep it constant. This is rarely possible in most practical applications and, in particular, when conducting in-field inspection. If the standoff distance is constantly measured during a scan (mechanically, electrically, or optically), then by knowing the relationship between the standoff distance and the output of the probe, one may compensate for the adverse effect of standoff distance change (not unlike the compensating method described previously) [32]. Compensation in this case is referred to as removing or reducing the adverse effect of standoff distance change from the output of the probe.

Subsequently, a novel millimeter wave dual differential probe was proposed, designed, and developed for the purpose of detecting very small corrosion pitting under paint while keeping the adverse influence of clutter—most notably standoff distance variation—to a minimum [49]. The picture of this novel millimeter wave dual differential probe is shown in Figure 6. As can been seen in Figure 6(a), this probe consists of a millimeter wave source (oscillator), a magic tee, two identical waveguide aperture probes, and a detector. The separate machined waveguide structure and magic tee are shown in Figure 6(b). A continuous wave (CW) oscillator, such as a Gunn oscillator, is used to generate a signal in the V-band frequency range (50–75 GHz) which is then fed to the sum port of the magic tee through an isolator that prevents unwanted reflections from entering the oscillator.

Since the two waveguide apertures of the dual differential probe are adjacent to each other, the dual differential probe senses the difference between reflected signals from close areas on the test specimen. While scanning a test specimen, if the two reflected signals are identical in magnitude and phase (e.g., the two waveguide apertures are probing areas with identical features), then the input signal to the

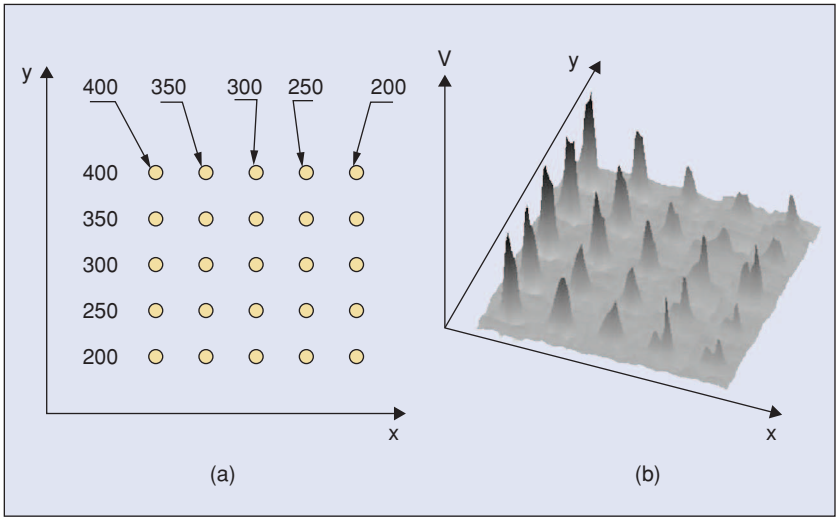

Fig. 5. (a) Schematic of the laser-pitted plate (the horizontal and vertical numbers show dimensions in μm of diameter and depth of pittings, respectively) and (b) an image of the pittings at 67 GHz. The height of the picks is proportional to the output voltage, *V*, of the probe. Reprinted with permission from M. Ghasr, S. Kharkovsky, R. Zoughi, and R. Austin from *Review of Progress in Quantitative Nondestructive Evaluation* 25B, AIP Conference Proceedings, vol.760, pp. 547–553, 2005, Copyright 2006, American Institute of Physics.

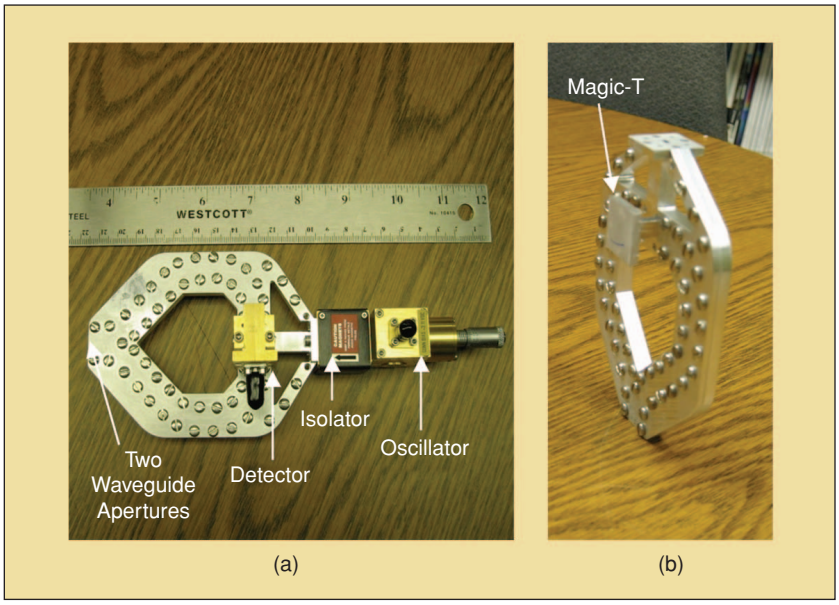

Fig. 6. Picture of (a) the millimeter wave dual differential probe and (b) its machined waveguide structure and magic tee [90].

detector will be zero (i.e., coherent difference between these two reflected signals), resulting in no detector output voltage. However, when one of the waveguide apertures senses a small localized target such as a pitting, the signal input to the detector will no longer be zero and the detector produces a voltage proportional to the magnitude of the difference signal. Also, when detecting a pitting, it is first detected by one of the waveguide probes and then, as the scan continues, by the other probe. Since the reflected signals from these two probes at any given time are subtracted from one another, the outcome of imaging a pitting will be two images of the pitting next to one another and with opposite intensity contrasts [49].

In some cases, microwave and millimeter wave NDT&E techniques may be the only viable solution or can be used in combination with other methods to render a more comprehensive picture for an inspection problem.

Several aluminum panels containing pitting of various sizes and properties were investigated by this probe. One of these panels had a set of laser-machined pittings with openings (diameters) and depths ranging from 100–500 μm covered by a thin layer of appliqué (paint like polymer). Figure 7 shows the image of three of these pittings in the form of dual indications of opposite intensity contrasts with a clear background, as expected (i.e., no indication of standoff distance variation). This image represents the raw data obtained from the dual differential probe without any signal or image processing. These pittings were previously imaged using a single probe, where the image was severely affected by the presence of edge effect [48].

It is important to note that, using calibrated pittings (i.e., laser pittings whose depths and widths are reasonably accurately known) and a smart decision-making process (such as a fuzzy logic algorithm), it is also possible to obtain a close estimate of a given pit size once it has been detected [90], [91]. This is an important issue since, once a pitting is detected (under paint or when exposed), it may be sanded off to eliminate a potential stress point on the structure. However, how much to sand off and whether the pitting is deep enough to require a more significant rehabilitation process depends on close determination of its depth.

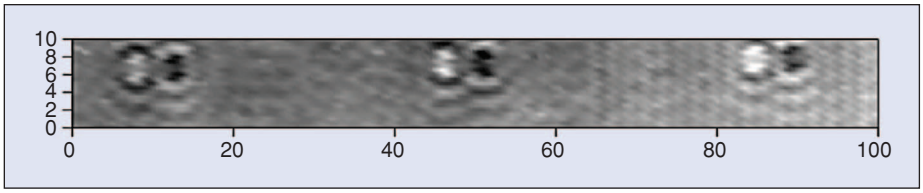

Fig. 7. Millimeter wave images of three pits 500 μm in diameter and depths of (from left to right) 150, 200, and 500 μm under appliqué obtained at 67 GHz using the dual differential probe. Dual indications of opposite intensity correspond to each pit. Reprinted with permission from M. Ghasr, B. Carroll, S. Kharkovsky, R. Zoughi, and R. Austin from *IEEE Transactions on Instrumentation and Measurement*, vol. 55, no. 5, pp. 1620–1627, October 2006, Copyright 2006, IEEE.

Inspection of Spray-On Foam Insulation on the Space Shuttle External Fuel Tank

The Space Shuttle Columbia Accident Investigation Board (CAIB) report has pointed to a flyaway section of spray-on foam insulation (SOFI) from the left bipod fairing on the external fuel tank as the cause of the Space Shuttle Columbia's failure during reentry into the atmosphere [92]. Some critical foam loss regions of the external tank are structurally complex in geometry and design. Therefore, any NDT&E technique used for inspecting the state of the foam must be able to overcome many limiting issues that are created by this complexity. Additionally, this insulating closed-cell foam material is by nature low density and may be as thick as 23 cm in some regions of the tank, which consequently presents many of the standard NDT&E techniques with significant challenges for a robust inspection. In the microwave and millimeter wave frequency ranges, the low-density nature of the foam and its polymeric makeup translate to a low dielectric permittivity and loss factor. In other words, the difference between the dielectric properties of the foam and anomalies, such as voids or disbonds, is small. For example, the (relative-to-air) dielectric properties of a typical piece of SOFI were measured at 10 GHz to be approximately (1.05 – j0.003) [50]. Subsequently, when using these frequencies, sensitive inspection systems must be carefully designed in such a way that the presence of these "weak scattering" anomalies can still be detected.

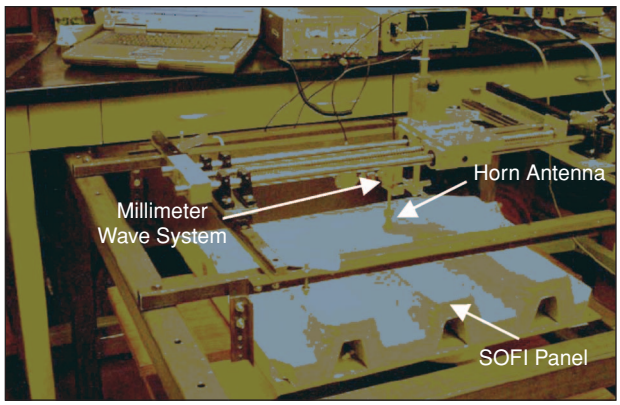

Fig. 8. Picture of the 100-GHz reflectometer with a small horn antenna testing the SOFI panel. From *Materials Evaluation*, vol. 63, no. 5. Reprinted with permission of the American Society for Nondestructive Testing, Inc.

An advantage of high-frequency measurements is the inherent capability of obtaining high-resolution images when imaging a structure.

Clearly, unlike other applications mentioned earlier, imaging SOFI cannot be performed using near-field techniques. Moreover, whatever the technique, it must provide for a very fine spatial resolution (in the order of a few mm). Therefore, these requirements dictate that the imaging system must operate at higher millimeter wave frequencies and be capable of focusing (real or synthetic) the interrogating beam on a very small spot. To this end, several millimeter wave reflectometers were designed and tested on various SOFI panels. These reflectometers operated in a wide range of frequencies from 24-150 GHz. Small horn antennas as well as dielectric lens antennas were incorporated into these systems for obtaining small inspection footprints and, hence, finer spatial resolutions [50]–[52], [93]. In another extensive investigation, the utility of synthetic aperture imaging and holography for obtaining high-resolution images of SOFI was also investigated with much success [53], [94], [95].

Currently, the most prominent on-site methods for detecting disbonds and other defects or anomalies such as cracks, impact damages, fiber breakages, and fiber misalignment are visual inspection and tap testing.

Imaging Using Real Aperture Focusing Techniques

We designed a reflectometer system operating at 100 GHz and composed of mono-static transmitting and receiving millimeter wave sections. The transmitted and received signals correspond to the same illuminated areas/volumes, unlike a bistatic measurement system in which separate transmitting and receiving antennas are required. Careful design of such monostatic systems can also produce images that are both phase and magnitude sensitive [2]. This is important since, depending on the dielectric properties of the structure under inspection and the type of anomaly that may exist in the structure, the phase or magnitude of the reflected signal from an anomaly may be a better indicator of its presence and properties. Subsequently, both a small horn antenna and a focused lens antenna were used to produce images of several SOFI panels with various embedded anomalies representing voids and disbonds. The lens antenna had a focal length of 25.4 cm with a corresponding footprint of 1.25 cm at this distance.

When inspecting panels with stringers, images were produced using two distinct incident signal polarizations: namely, one in which the incident electric field polarization vector was parallel to the stringer axes (referred to as the parallel polarization) and one where this vector was perpendicular to the stringer axes (referred to as the perpendicular polarization). Polarization diversity, which is a significant attribute of these millimeter wave measurements, can provide images possessing different and complementary information about a particular anomaly when the anomaly is located near a structural member that has a preferred orientation with respect to the polarization vector direction. The structural members in this case include stringers, flanges, bolts, etc. Figure 8 shows a picture of the millimeter wave system at 100 GHz using a small horn antenna scanning an SOFI panel used in this investigation.

Several panels were used in this study. These panels collectively provided for different and important geometries related to the complex structural properties of the external tank as well as different types of anomalies that may be encountered. The results for one specific panel are presented here. This panel was designed to resemble the intertank flange portion of the fuel tank and consisted of three stringers, a flange, and three bolts through the flange centered in front of the stringer openings. The aluminum substrate thickness was 0.63 cm. Figure 9(a) shows a picture of this panel prior to the application of the SOFI. Several rubber inserts and SOFI void inserts were placed at critical regions of this panel, as shown in Figure 9(a). The rubber anomalies are not expected to be found in an external tank structure and were used here only for comparative purposes with the SOFI voids. The SOFI was subsequently sprayed on this panel and the foam surface was then trimmed in a manner similar to the external tank intertank flange close-out. Consequently, this panel possessed foam thickness ranging

Fig. 9. The SOFI panel picture (a) before (white circles are SOFI void inserts and black squares are rubber inserts) and (b) after SOFI application. From *Materials Evaluation*, vol. 63, no. 5. Reprinted with permission of the American Society for Nondestructive Testing, Inc.

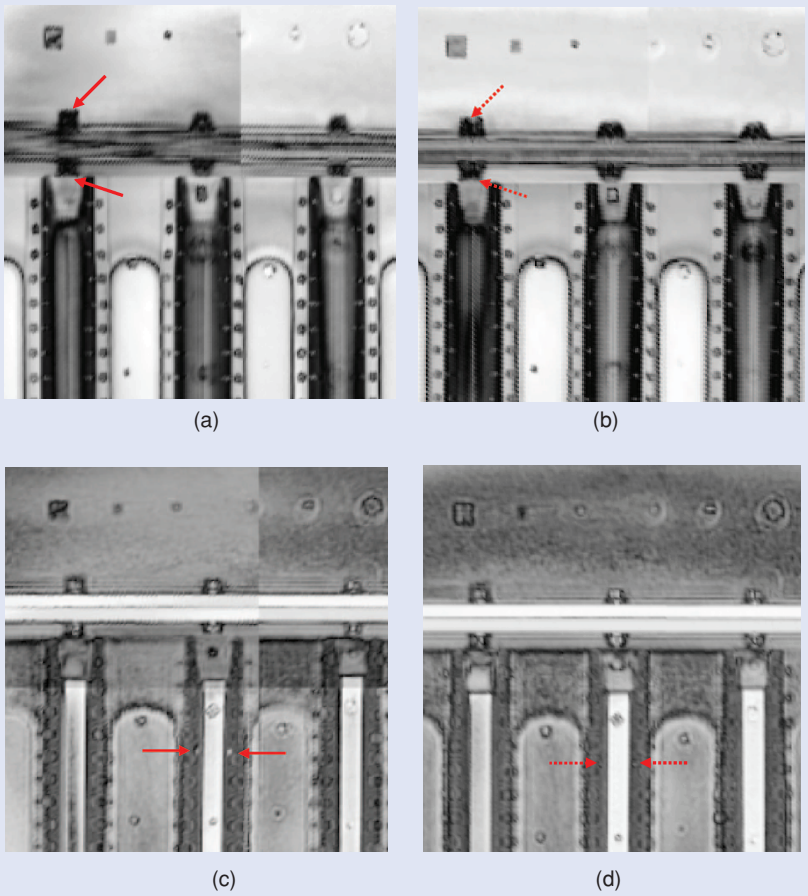

Fig. 10. 100-GHz image of the SOFI panel with lens focused on the aluminum substrate at (a) parallel polarization and (b) perpendicular polarization (red arrows show the indications of inserts below the left bolt) and with the lens focused on the top of the stringers at (c) parallel polarization and (d) perpendicular polarization (red arrows show the indications of inserts on the sides of the middle stringer). Reprinted with permission from R. Zoughi, S. Kharkovsky, and F. Hepburn from *Review of Progress in Quantitative Nondestructive Evaluation* 25B, AIP Conference Proceedings, vol.820, pp. 439-446, 2006, Copyright 2006, American Institute of Physics.

from 2.54–10 cm over different regions. Additionally, the foam on the top portion of the panel was in the form of a ramp that varied in thickness from 7.62 cm to about 3.1 cm. Figure 9(b) shows a picture of this panel.

Figure 10(a)–(d) shows the parallel and perpendicular polarization images of this panel at 100 GHz when the lens was focused at the substrate and on the top of the stringers, respectively. From these images, one can see that most of the inserts were detected [93]. It is important to note that Figure 10(a) and 10(b) clearly shows impressions of the rubber inserts below the left bolt and Figure 10(c) and (d) clearly shows the rubber inserts on the sides of the middle stringer. The regions of the side and openings stringers and regions of the bolts and flanges are most critical for detection of SOFI anomalies. It is also evident that the parallel polarization results show the inserts on the sides of the stringer (marked by solid red arrows) much better than the perpendicular polarization results (marked by dot red arrows) as described earlier.

Synthetic Aperture Focusing and Holography

There is an ever-increasing demand for producing images with finer resolutions. The use of highly focused lenses can produce fine spatial resolution, while incorporating a pulsed or swept frequency system into the overall imaging system can render fine depth resolution (i.e., in the direction of signal propagation). In the microwave and millimeter wave regime, it may be easier to sweep the frequency rather than produce a very narrow pulsed signal. However, the use of a wide-band system is not consistent with a lens that focuses the beam to a very narrow beam at a particular frequency. Therefore, to overcome some of these limitations and still produce a three-dimensional (3-D) high-resolution image, one may use synthetic aperture focusing and holographic techniques. These methods have been used for various imaging purposes, including detection of concealed weapons, imaging of the Space Shuttle SOFI, and acreage heat tiles [53], [93]–[97]. The reader is encouraged to review these references and many other articles published in this area.

Conclusions

This article briefly introduced the science of NDT&E while focusing on the unique methods involving microwave and millimeter wave technologies. There has been an increase in scientific investigation and hardware development in this area in the past 20 years. The three examples of applications presented in this article are not all-inclusive in terms of the areas of applicability and the investigating groups that are involved in these areas. Given the past history of these methods and the future outlook for more incorporation of composite materials in a wide range of structures, the future of microwave and millimeter wave NDT&E is bright in regard to its utility, usefulness, hardware development, and commercialization of new systems. The inadequate commercial availability of microwave and millimeter wave systems for NDT&E purposes has limited its more extensive implementation. However, we envision that this inadequacy will become less of a limiting issue in the next decade.

Acknowledgements

Portions of the "Inspection of Carbon Fiber Reinforced Polymer Composite Laminate-Strengthened Structural Members" section are reprinted with permission from S. Kharkovsky, A.C. Ryley, V. Stephen, and R. Zoughi, *Proc. IEEE Instrumentation and Measurement Technology Conf.*, Sorrento, Italy, 2006, pp. 2108–2111, Copyright 2006 IEEE.

Portions of the "Detection and Evaluation of Corrosion and Precursor Pitting Under Paint" section are reprinted with permission from S. Kharkovsky and R. Zoughi, *Review of Progress in Quantitative Nondestructive Evaluation 25B, AIP Conference Proceedings*, 2006, vol. 820, pp. 1277–1283, Copyright 2006, American Institute of Physics, and with permission from M. Ghasr, B. Carroll, S. Kharkovsky, R. Zoughi, and R. Austin, *IEEE Transactions on Instrumentation and Measurement*, vol. 55, no. 5, pp. 1620–1627, October 2006, Copyright 2006 IEEE.

Portions of the "Inspection of Spray-On-Foam Insulation on the Space Shuttle External Fuel tank" section are from *Materials Evaluation*, vol. 63, no. 5. Reprinted with permission of the American Society for Nondestructive Testing, Inc.; reprinted with permission from R. Zoughi, S. Kharkovsky, and F.L. Hepburn, *Review of Progress in Quantitative Nondestructive Evaluation* 25B, AIP Conference Proceedings, vol. 820, 2006, pp. 439–446, Copyright 2006, American Institute of Physics.

References

[1] P.J. Shull, *Nondestructive Evaluation: Theory, Techniques, and Applications*. New York: Marcel Dekker, 2002.

[2] R. Zoughi, *Microwave Non-Destructive Testing and Evaluation*. The Netherlands: Kluwer, 2000.

[3] D.M. Pozar, *Microwave Engineering*, 2nd ed. New York: Addison Wesley, 1990.

[4] A.J. Bahr, *Microwave Nondestructive Testing Methods*. Newark, NJ: Gordon and Breach, 1982.

[5] A. Sihvola, *Electromagnetic Mixing Formulas and Applications* (IEE Electromagnetic Series 47). London, U.K.: IEE Publishers, 1999.

[6] S. Gray, S. Ganchev, N. Qaddoumi, G. Beauregard, D. Radford, and R. Zoughi, "Porosity level estimation in polymer composites using microwaves," *Materials Eval.*, vol. 53, no. 3, pp. 404–408, Mar. 1995.

[7] S. Ganchev, N. Qaddoumi, D. Brandenburg, S. Bakhtiari, R. Zoughi, and J. Bhattacharyya, "Microwave diagnosis of rubber compounds," *IEEE Trans. Microwave Theory Tech.*, vol. 42, no. 1, pp. 18–24, Jan. 1994.

[8] W. Shalaby and R. Zoughi, "Analysis of monopole sensors for cement paste compressive strength estimation," *Res. Nondestruct. Eval.*, vol. 7, no. 2/3, pp. 101–105, 1995.

[9] K.J. Bois, A. Benally, P.S. Nowak, and R. Zoughi, "Microwave nondestructive determination of sand to cement (s/c) ratio in mortar," *Res. Nondestruct. Eval.*, vol. 9, no. 4, pp. 227–238, 1997.

[10] K.J. Bois, A. Benally, P.S. Nowak, and R. Zoughi, "Cure-state monitoring and water-to-cement ratio determination of fresh Portland cement based materials using near field microwave techniques," *IEEE Trans. Instrum. Meas.*, vol. 47, no. 3, pp. 628–637, June 1998.

[11] S. Kharkovsky, M.F. Akay, U.C. Hasar, and C.D. Atis, "Measurement and monitoring of microwave reflection and transmission properties of cement-based specimens," *IEEE Trans. Instrum. Meas.*, vol. 51, no. 6, pp. 1210–1218, Dec. 2002.

[12] K.J. Bois, L. Handjojo, A. Benally, K. Mubarak, and R. Zoughi, "Dielectric plug-loaded two-port transmission line measurement technique for dielectric property characterization of granular and liquid materials," *IEEE Trans. Instrum. Meas.*, vol. 48, no. 6, pp. 1141–1148, Dec. 1999.

[13] K.J. Bois, A. Benally, and R. Zoughi, "Microwave near-field reflection property analysis of concrete for material content determination," *IEEE Trans. Instrum. Meas.*, vol. 49, no. 1, pp. 49–55, Feb. 2000.

[14] L. Handjojo, K.J. Bois, J. Bauer, R. Hamilton, and R. Zoughi, "Broad-band microwave dielectric property characterization of various glass specimens," *Nondestruct. Testing Eval.*, vol. 16, pp. 55–69, 2000.

[15] N. Qaddoumi, S. Ganchev, and R. Zoughi, "Microwave diagnosis of low density glass fibers with resin binder," *Res. Nondestruct. Eval.*, vol. 8, no. 3, pp. 177–188, 1996.

[16] K. Mubarak, K.J. Bois, and R. Zoughi, "A simple, robust and _on-site microwave technique for determining water-to-cement (w/c) ratio of fresh Portland cement-based materials," *IEEE Trans. Instrum. Meas.*, vol. 50, no. 5, pp. 1255–1263, Oct. 2001.

[17] K.J. Bois, A. Benally, and R. Zoughi, "Near-field microwave non-invasive determination of NaCl in mortar," *IEE Proc. Science, Measurement Technol. (Special Issue on Non-destructive Testing and Evaluation)*, vol. 148, no. 4, pp. 178–182, July 2001.

[18] S. Trabelsi, A. Kraszewski, and S. Nelson, "Simultaneous determination of density and water content of particulate materials by microwave sensors," *Electronic Lett.*, vol. 33, no. 10, pp. 874–876, 1997.

[19] S. Peer, K.E. Kurtis, and R. Zoughi, "An electromagnetic model for evaluating temporal water content distribution and movement in cyclically soaked mortar," *IEEE Trans. Instrum. Meas.*, vol. 53, no. 2, pp. 406–415, Apr. 2004.

[20] S. Peer, J.T. Case, E. Gallaher, K.E. Kurtis, and R. Zoughi, "Microwave reflection and dielectric properties of mortar subjected to compression force and cyclically exposed to water and sodium chloride solution," *IEEE Trans. Instrum. Meas.*, vol. 52, no. 1, pp. 111–118, Feb. 2003.

[21] D. Hughes and R. Zoughi, "A novel method for determination of dielectric properties of materials using a combined embedded modulated scattering and near-field microwave techniques. Part I—Forward model," *IEEE Trans. Instrum. Meas.*, vol. 54, no. 6, pp. 2389–2397, Dec. 2005.

[22] D. Hughes and R. Zoughi, "A novel method for determination of dielectric properties of materials using a combined embedded modulated scattering and near-field microwave techniques. Part II—Dielectric property recalculation," *IEEE Trans. Instrum. Meas.*, vol. 54, no. 6, pp. 2398–2401, Dec. 2005.

[23] M.C. Decreton and F.E. Gardiol, "Simple nondestructive method for measurement of complex permittivity," *IEEE Trans. Instrum. Meas.*, vol. IM-23, no. 6, pp. 434–438, Dec. 1974.

[24] S. Bakhtiari and R. Zoughi, "Microwave thickness measurement of lossy layered dielectric slabs using incoherent reflectivity," *Res. Nondestruct. Eval.*, vol. 2, no. 3, pp. 157–168, 1990.

[25] S. Bakhtiari, S. Ganchev, and R. Zoughi, "Open-ended rectangular waveguide for nondestructive thickness measurement and variation detection of lossy dielectric slabs backed by a conducting plate," *IEEE Trans. Instrum. Meas.*, vol. 42, no. 1, pp. 19–24, Feb. 1993.

[26] S. Bakhtiari, S. Ganchev, N. Qaddoumi, and R. Zoughi, "Microwave non-contact examination of disbond and thickness variation in stratified composite media," *IEEE Trans. Microwave Theory Tech.*, vol. 42, no. 3, pp. 389–395, Mar. 1994.

[27] S. Ganchev, N. Qaddoumi, E. Ranu, and R. Zoughi, "Microwave detection optimization of disbond in layered dielectrics with varying thicknesses," *IEEE Trans. Instrum. Meas.*, vol. IM-44, no. 2, pp. 326–328, Apr. 1995.

[28] S. Ganchev, N. Qaddoumi, S. Bakhtiari, and R. Zoughi, "Calibration and measurement of dielectric properties of finite thickness composite sheets with open-ended coaxial sensors," *IEEE Trans. Instrum. Meas.*, vol. IM-44, no. 6, pp. 1023–1029, Dec. 1995.

[29] S. Bakhtiari, S. Gopalsami, and A.C. Raptis, "Characterization of delamination and disbonding in stratifies dielectric composites by millimeter wave imaging," *Materials Eval.*, vol. 53, no. 4, pp. 468–471, Apr. 1995.

[30] N. Qaddoumi, R. Zoughi, and G.W. Carriveau, "Microwave detection and depth determination of disbonds in low-permittivity and low-loss thick sandwich composites," *Res. Nondestruct. Eval.*, vol. 8, no. 1, pp. 51–63, 1996.

[31] S. Gray and R. Zoughi, "Dielectric sheet thickness variation and disbond detection in multi-layered composites using an extremely sensitive microwave approach," *Materials Eval.*, vol. 55, no. 1, pp. 42–48, 1997.

[32] N. Qaddoumi, T. Bigelow, R. Zoughi, L. Brown, and M. Novack, "Reduction of sensitivity to surface roughness and slight standoff distance variations in microwave inspection of thick composite structures," *Materials Eval.*, vol. 60, no. 2, pp. 165–170, Feb. 2002.

[33] A.J. Bahr, "Microwave eddy-current techniques for quantitative nondestructive evaluation," in *Eddy-Current Characterization of Materials and Structures* (ASTM STP 722), G. Birnbaum and G. Free, Eds., Philadelphia, PA: American Society for Testing and Materials, pp. 311–331, 1981.

[34] B.A. Auld, "*Theory of ferromagnetic resonance probes for surface cracks in metals*," E.L. Ginzton Lab., Stanford University, Stanford, CA, G.L. rep. 2839, July 1978.

[35] N. Qaddoumi, E. Ranu, J.D. McColskey, R. Mirshahi, and R. Zoughi, "Microwave detection of stress induced fatigue cracks in steel and potential for crack opening determination," *Res. Nondestruct. Eval.*, vol. 12, no. 2, pp. 87–103, 2000.

[36] C. Yeh and R. Zoughi, "A novel microwave method for detection of long surface cracks in metals," *IEEE Trans. Instrum. Meas.*, vol. 43, no. 5, pp. 719–725, Oct. 1994.

[37] C. Yeh, and R. Zoughi, "Sizing technique for surface cracks in metals," *Materials Eval.*, vol. 53, no. 4, pp. 496–501, Apr. 1995.

[38] C. Huber, H. Abiri, S. Ganchev, and R. Zoughi, "Analysis of the crack characteristic signal using a generalized scattering matrix representation," *IEEE Trans. Microwave Theory Tech.*, vol. 45, no. 4, pp. 477–484, Apr. 1997.

[39] C. Huber, H. Abiri, S. Ganchev, and R. Zoughi, "Modeling of surface hairline crack detection in metals under coatings using open-ended rectangular waveguides," *IEEE Trans. Microwave Theory Tech.*, vol. 45, no. 11, pp. 2049–2057, Nov. 1997.

[40] K. Haddadi, D. Glay, and T. Lasri, "Homodyne dual six-port network analyzer and associated calibration technique for millimeter wave measurements," in *Proc. IEEE Int. Symp. Circuits and Systems*, pp. 4, May 21–24, 2006.

[41] F. Mazlumi, S.H.H. Sadeghi, and R. Moini, "Interaction of an open-ended rectangular waveguide probe with an arbitrary-shape surface crack in a lossy conductor," *IEEE Trans. Microwave Theory Tech.*, vol. 54, no. 10, pp. 3706–3711, Oct. 2006.

[42] N. Wang and R. Zoughi, "Moment method solution for modeling the interaction of open-ended coaxial probes and surface cracks in metals," *Materials Eval.*, vol. 60, no. 10, pp. 1253–1258, Oct. 2002.

[43] Y. Wang and R. Zoughi, "Interaction of surface cracks in metals with open-ended coaxial probes at microwave frequencies," *Materials Eval.*, vol. 58, no. 10, pp. 1228–1234, Oct. 2000.

[44] R. Zoughi, C. Huber, N. Qaddoumi, E. Ranu, V. Otashevich, R. Mirshahi, S. Ganchev, and T. Johnson, "Real-time and on-line microwave inspection of surface defects in rolled steel," in *Proc. Asia-Pacific Microwave Conf. (APMC'97)*, Hong Kong, pp. 1081–1084, Dec. 2–5, 1997.

[45] N. Qaddoumi, A. Shroyer, and R. Zoughi, "Microwave detection of rust under paint and composite laminates," *Res. Nondestruct. Eval.*, vol. 9, no. 4, pp. 201–212, 1997.

[46] N. Qaddoumi, L. Handjojo, T. Bigelow, J. Easter, A. Bray, and R. Zoughi, "Microwave corrosion detection using open-ended rectangular waveguide sensors," *Materials Eval.*, vol. 58, no. 2, pp. 178–184, Feb. 2000.

[47] D. Hughes, N. Wang, T. Case, K. Donnell, R. Zoughi, R. Austin, and M. Novack, "Microwave nondestructive detection of corrosion under thin paint and primer in aluminum panels," *Subsurface Sensing Technol. Applicat: An Int. J. (Special Issue on Advances Applications in Microwave and Millimeter Wave Nondestructive Evaluation*), vol. 2, no. 4, pp. 435–451, 2001.

[48] M. Ghasr, S. Kharkovsky, R. Zoughi, and R. Austin, "Comparison of near-field millimeter wave probes for detecting corrosion precursor pitting under paint," *IEEE Trans. Instrum. Meas.*, vol. 54, no. 4, pp. 1497–1504, Aug. 2005.

[49] M. Ghasr, B.J. Carroll, S. Kharkovsky, R. Zoughi, and R. Austin, "Millimeter wave differential probe for nondestructive detection of corrosion precursor pitting," *IEEE Trans. Instrum. Meas.*, vol. 55, no. 5, pp.1620–1627, Oct. 2006,.

[50] S. Shrestha, S. Kharkovsky, R. Zoughi, and F. Hepburn, "Microwave and millimeter wave nondestructive evaluation of the Space Shuttle external tank insulating foam," *Materials Eval.*, vol. 63, no. 3, pp. 339–344, Mar. 2005.

[51] S. Kharkovsky, F. Hepburn, J. Walker, and R. Zoughi, "Testing of the Space Shuttle external tank SOFI using near-field and focused millimeter wave nondestructive testing techniques," *Materials Eval.*, vol. 63, no. 5, pp. 516–522, May 2005.

[52] S. Kharkovsky, J.T. Case, M.A. Abou-Khousa, R. Zoughi, and F. Hepburn, "Millimeter wave detection of localized anomalies in the Space Shuttle external fuel tank insulating foam," *IEEE Trans. Instrum. Meas.*, vol. 55, no. 4, pp. 1250–1257, Aug. 2006.

[53] J.T. Case, F. Hepburn, and R. Zoughi, "Inspection of spray on foam insulation (SOFI) using microwave and millimeter wave synthetic aperture focusing and holography," in *Proc. IEEE Instrumentation and Measurement Technology Conf. (IMTC06)*, Sorrento, Italy, pp. 2148–2153, April 24–27, 2006.

[54] R. Koganti and R. Zoughi, "Three dimensional numerical simulation of microwave imaging based on an iterative forward reconstruction method," *Materials Eval.*, vol. 64, no. 10, pp. 1014–1019, Oct. 2006.

[55] S. Caorsi, A. Massa, M. Pastorino, and A. Randazzo, "Electromagnetic detection of dielectric scatterers using phaseless synthetic and real data and the memetic algorithm," *IEEE Trans. Geoscience Remote Sensing*, vol. 41, no. 12, pp. 2745–2753, Dec. 2003.

[56] M. Pastorino, "A microwave inverse scattering technique for image reconstruction based on a genetic algorithm," *IEEE Trans. Instrum. Meas.*, vol. 49, no. 3, pp. 573–578, June 2000.

[57] S. Caorsi, S. Ciaramella, G.L. Gragnani, and M. Pastorino, "On the use of regularization techniques in numerical inverse-scattering solutions for microwave imaging applications," *IEEE Trans. Microwave Theory Tech.*, vol. 43, no. 3, pp. 632–640, Mar. 1995.

[58] J.C. Bolomey, "Recent European developments in active microwave imaging for industrial, scientific and medical applications," *IEEE Trans. Microwave Theory Tech.*, vol. 37, no. 12, pp. 2109–2117, Dec. 1989.

[59] A. Franchois and C. Pichot, "Microwave imaging-complex permittivity reconstruction with Levenberg-Marquardt method," *IEEE Trans. Antennas Propagat.*, vol. 45, pp. 203–215, Feb. 1997.

[60] M. Stuchly and S. Stuchly, "Coaxial line reflection methods for measuring dielectric properties of biological substances at radio and microwave frequencies—A review," *IEEE Trans. Instrum. Meas.*, vol. IM-29, no. 3, pp. 176–183, Sept. 1980.

[61] E.C. Fear, S.C. Hagness, P.M. Meaney, M. Okoniewski, and M.A. Stuchly, "Enhancing breast tumor detection with near-field imaging," *IEEE Microwave Mag.*, vol. 3, pp. 48–56, Mar. 2002.

[62] P. Mehta, K. Chand, D. Narayanswamy, D.G. Beetner, R. Zoughi, and W.V. Stoeker, "Microwave reflectometry as a novel diagnostic tool for detection of skin cancers," *IEEE Trans. Instrum. Meas.*, vol. 55, no. 4, pp. 1309–1316, Aug. 2006.

[63] S. Hagness, A. Taflove, and J. Bridges, "Three-dimensional FDTD analysis of a pulsed microwave confocal system for breast cancer detection: Design of an antenna—Array element," *IEEE Trans. Antennas Propagat.*, vol. 47 no. 5, pp. 783–791, May 1999.

[64] E.C. Fear, X. Li, S.C. Hagness, and M.A. Stuchly, "Confocal microwave imaging for breast cancer detection: Localization of tumors in three dimensions," *IEEE Trans. Biomed. Eng.*, vol. 49, no. 8, pp. 812–822, Aug. 2002.

[65] D.W. Winters, E.J. Bond, B.D. Van Veen, and S.C. Hagness, "Estimation of the frequency-dependent average dielectric properties of breast tissue using a time-domain inverse scattering technique," *IEEE Trans. Antennas Propagat.*, vol. 54, no. 11, pp. 3517–3528, Nov. 2006.

[66] W.T. Joines, S. Shrivastav, and R.L. Jirtle, "A comparison using tissue electrical properties and temperature rise to determine relative absorption of microwave power in malignant tissue," *Medical Physics*, vol. 16, no. 6, pp. 840–844, Dec. 1989.

[67] M. Tabib-Azar, A. Garcia-Valenzuela, and G. Ponchak, *Evanescent Microwave Microscopy for High Resolution Characterization of Materials*. Norwell, MA: Kluwer, 2002.

[68] B.T. Rosner, and D.W. Van der Weide, "High-frequency near-field microscopy," *Rev. Scientific Instrum.*, vol. 73, no. 7, pp. 2505–2525, 2002.

[69] S. Kim, H. Yoo, K. Lee, B. Friedman, M.A. Gaspar, and R. Levicky, "Distance control for near-field scanning microwave microscope in liquid using a quartz tuning fork," *Applied Physics Lett.*, vol. 86, article 153506, Apr. 2005 [Online]. Available: http://apl.aip.org

[70] A. Nanni,"North American design guidelines for concrete reinforcement and strengthening using FRP: Principles, applications, and unresolved issues," *Construction and Building Materials,* vol. 17, no. 6-7, pp. 439-446, Sept.-Oct. 2003.

[71] B. Taljsten, "Strengthening of concrete structures for shear with bonded CFRP fabrics," in *Proc. U.S.-Canada-Europe Workshop Recent Advances Bridge Engineering*, U. Meier and R. Betti, Eds. , Dübendorf, Switzerland, 1997, pp. 67–74.

[72] F.W. Klaiber, T.J. Wipf, and B.J. Kempers., "Repair of damaged prestressed concrete bridges using CFRP," in *Proc. 2003 Mid-Continental Transportation Research Symp.*, Ames, Iowa, Aug. 2003 [Online]. Available: http://www.citre.iastate.edu/PUBS/midcon2003/KlaiberCFRP.pdf

[73] J.W. Littles, L. Jacobs, and A. Zureik, "Ultrasonic characterization of FRP composites for bridge applications," in *Proc. 11th Engineering Mechanics Conf.*, Fort Lauderdale, Florida, vol. 2, pp. 956–962, 1996.

[74] D.G. Mandic, R.E. Martin, and J.H. Hermann, "Thermal imaging technique to detect delaminations in CFRP plated concrete," in *Proc. Nondestructive Evaluation of Materials Composites*, Int. Soc. for Optical Engineering, San Antonio, Texas, vol. 3396, pp. 22–27, 1998.

[75] W. Tawhed and S. Gassman, "Damage assessment of concrete bridge decks using impact-echo method," *ACI Materials J.*, vol. 99, no. 30, pp.273–281, 2002.

[76] J. Shih, D. Tann, C. Hu, R. Delpak, and E. Andreou, "Remote sensing of air blisters in concrete-FRP bond layer using IR thermography," *Int. J. Materials Production Technol.*, vol. 19, no. 1-2, pp.174–187, 2003.

[77] H. Yang, A. Nanni, S. Haug, and C.L. Sun, "Strength and modulus degradation of carbon fiber-reinforced polymer laminates from fiber misalignment," *ASCE J. Materials Civil Eng.*, vol.14, no. 4, pp. 320–326, 2002.

[78] N.F. Declercq, A. Tekulu, M.A. Breazeale, R.D. Hasee, J. Degrieck, and O. Leroy, "Detection of fiber direction in composites by means of a high-frequency wide-bounded ultrasonic beam and Schlieren photography," *Res. Nondestruct. Eval.*, vol. 16, no. 2, pp. 55–64, 2005.

[79] M.Q. Feng, F.D. Flaviis, and Y.J. Kim, "Use of microwaves for damage detection of fiber reinforced polymer-wrapped concrete structures," *J. Eng. Mech.*, vol. 128, no. 2, pp.172–183, 2002.

[80] O. Buyukozturk, J. Park, and C. Au, "Non-destructive evaluation of FRP-confined concrete using microwaves," in *Proc. Int. Symp. Non-Destructive Testing in Civil Engineering, Berlin*, Sept. 16–19, 2003 [Online]. Available: http://www.ndt.net/article/ndtce03/papers/v085/v085.htm

[81] Y.J. Kim, L. Jofre, F.D. Flaviis, and M.Q. Feng, "Microwave subsurface imaging technology for damage detection," *J. Eng. Mech.*, vol. 130, no. 7, pp. 858–866, July 2004.

[82] B. Akuthota, D. Hughes, R. Zoughi, and J. Myers, "Near-field microwave detection of disbond in fiber reinforced polymer composites used for strengthening concrete structures and disbond repair verification," *ASCE J. Materials Civil Eng.*, vol.16, no. 6, pp. 540–546, 2004.

[83] V. Stephen, S. Kharkovsky, J. Nadakuduti, and R. Zoughi, "Microwave field measurement of delaminations in CFRP concrete members in a bridge," in *Proc. World Conf. Nondestructive Testing (WCNDT)*, Montreal, Canada, pp. 5, Aug. 30–Sep. 3, 2004.

[84] S. Kharkovsky, A.C. Ryley, V. Stephen, and R. Zoughi, "Dual-polarized microwave near-field reflectometer for noninvasive inspection of carbon fiber reinforced polymer (CFRP) strengthened structures," in *Proc. IEEE Instrumentation and Measurement Technology Conf.*, Sorrento, Italy, pp. 2108–2111, 2006.

[85] R. Baboian, Ed., *Corrosion Tests and Standards: Application and Interpretation*. Philadelphia, PA: American Society for Testing and Materials, 1995.

[86] W. Funke, "Blistering of paint films," in *Corrosion Control by Organic Coatings*, Henry Leidheiser, Jr., Ed. Houston: Nat. Ass. Corrosion Engineers, pp. 97–102, 1981.

[87] J.A. Collins, *Failure of Materials in Mechanical Design*, 2nd ed. New York: Wiley Interscience, 1993.

[88] W.C. Fitzgerald, M.N. Davis, J.L. Blackshire, J.F. Maguire, and D.B. Mast, "Evanescent microwave sensor scanning for detection of subcoating corrosion," *J. Corrosion Science Eng.*, vol. 3, paper 15, 2001 [Online]. Available: http://www.jcse.org/Volume2/Paper15/v3p15.html

[89] S. Kharkovsky and R. Zoughi, "Millimeter wave nondestructive evaluation of corrosion under paint in steel structures," in *Review of Progress in Quantitative Nondestructive Evaluation* 25B, D.O. Thompson and D.E. Chimenti, Eds. Melville, NY: American Institute of Physics, 2006.

[90] M.T. Ghasr, "Detection and size evaluation of corrosion precursor pitting using near-field microwave and millimeter wave nondestructive testing methods," Master's thesis, Electrical and Computer Engineering Department, University of Missouri-Rolla, Rolla, MO, Oct. 2004.

[91] M. Ghasr, B. Carroll, S. Kharkovsky, R. Zoughi, and R. Austin, "Size evaluation of corrosion precursor pitting using near-field millimeter wave nondestructive testing methods," in *Proc. 31st Ann. Rev. Progress in Quantitative Nondestructive Evaluation*, vol. 760, pp. 547–553, 2005.

[92] Columbia Accident Investigation Board Report, NASA, Aug. 2003.

[93] R. Zoughi, S. Kharkovsky, and F. Hepburn, "Microwave and millimeter wave testing for the inspection of the Space Shuttle spray on foam insulation (SOFI) and the acreage heat tiles," in *Proc. 32nd Ann. Review of Progress in Nondestructive Evaluation*, vol. 25A, D.O. Thompson and D.E. Chimenti, Eds. AIP Conference Proc., vol. 820, pp. 439–446, 2006.

[94] J.T. Case, J. Robbins, S. Kharkovsky, R. Zoughi, and F. Hepburn, "Microwave and millimeter wave imaging of the Space Shuttle external tank spray on foam insulation (SOFI) using synthetic aperture focusing techniques (SAFT)," in *Proc. 32nd Ann. Review of Progress in Nondestructive Evaluation*, Brunswick, Maine, vol. 25B, pp. 1546–1553, July 31–Aug. 5, 2005.

[95] J.T. Case, "Microwave and millimeter wave imaging using synthetic aperture focusing and holographical techniques," Master's thesis, Electrical and Computer Engineering Department, University of Missouri-Rolla, Rolla, MO, Nov. 2005.

[96] D.M. Sheen, D.L. McMakin, and T.E. Hall, "Three-dimensional millimeter wave imaging for concealed weapon detection," *IEEE Trans. Microwave Theory Tech.*, vol. 49, no. 9, pp. 1581-1592, Sept. 2001.

[97] L.J. Busse, "Three-dimensional imaging using a frequency-domain synthetic aperture focusing technique," *IEEE Trans. Ultrasonic, Ferroelectrics, Freq. Control*, vol. 39, no. 2, pp. 174–179, Mar. 1992.

Sergey Kharkovsky (sergiy@umr.edu) is a research associate professor at the Applied Microwave Nondestructive Testing Laboratory (*amntl*) in the Electrical and Computer Engineering Department, University of Missouri-Rolla (UMR). Prior to joining UMR, he was a member of the research staff at the Institute of Radio-Physics and Electronics National Academy of Sciences of Ukraine and a professor in the Electrical and Electronics Engineering Department at the Cukurova University, Adana, Turkey. His current research interests are nondestructive testing and evaluation of composite structures and material characterization using microwaves and millimeter waves. He is a Senior Member of the IEEE.

Reza Zoughi (zoughir@umr.edu) is the Schlumberger Endowed Professor of Electrical and Computer Engineering at the University of Missouri-Rolla (UMR). Prior to joining UMR in January 2001, he was with the Electrical and Computer Engineering Department at Colorado State University (CSU), where he was a professor and established the Applied Microwave Nondestructive Testing Laboratory (*amntl*). He held the position of Business Challenge Endowed Professor of Electrical and Computer Engineering from 1995–1997 while at CSU. He is the editor-in-chief for *IEEE Transactions on Instrumentation and Measurement*. He is a Fellow of the American Society for Nondestructive Testing (ASNT) and an IEEE Fellow.